

# Chapter 2

## Protein Denaturation on $p$ - $T$ Axes – Thermodynamics and Analysis

László Smeller

**Abstract** Proteins are essential players in the vast majority of molecular level life processes. Since their structure is in most cases substantial for their correct function, study of their structural changes attracted great interest in the past decades. The three dimensional structure of proteins is influenced by several factors including temperature, pH, presence of chaotropic and cosmotropic agents, or presence of denaturants. Although pressure is an equally important thermodynamic parameter as temperature, pressure studies are considerably less frequent in the literature, probably due to the technical difficulties associated to the pressure studies.

Although the first steps in the high-pressure protein study have been done 100 years ago with Bridgman's ground breaking work, the field was silent until the modern spectroscopic techniques allowed the characterization of the protein structural changes, while the protein was under pressure.

Recently a number of proteins were studied under pressure, and complete pressure-temperature phase diagrams were determined for several of them. This review summarizes the thermodynamic background of the typical elliptic  $p$ - $T$  phase diagram, its limitations and the possible reasons for deviations of the experimental diagrams from the theoretical one. Finally we show some examples of experimentally determined pressure-temperature phase diagrams.

**Keywords** High pressure • Intrinsically disordered protein • Lysozyme • Myoglobin • Parvalbumin • Phase diagram • Ribonuclease • Rv3221c • Staphylococcal nuclease • Titin

### 2.1 Introduction

Proteins are one of the major constituents of the living matter. Since their structure is in most cases essential for their correct function, study of protein structure and dynamics attracted a lot of interest in the past decades. It is clear that the

---

L. Smeller (✉)

Department of Biophysics and Radiation Biology, Semmelweis University, Budapest, Hungary  
e-mail: [smeller.laszlo@med.semmelweis-univ.hu](mailto:smeller.laszlo@med.semmelweis-univ.hu)

three-dimensional structure of proteins is influenced by several physicochemical factors including temperature, pH, presence of chaotropic and kosmotropic agents, or presence of denaturants. All these are widely studied, but pressure, although it is another important thermodynamic parameter, is used in a significantly smaller amount of scientific publications. None of the physicists or chemists would treat pressure as less significant parameter than temperature, but the technical difficulties of pressure experiments could have prevented many scientists from the pressure studies.

Although Bridgman (1914), made the first steps in the high-pressure protein study 100 years ago the field was silent for a half of a century, and the research in the field started again with the seminal works of Kauzmann, Taniguchi and Suzuki (Suzuki 1960; Zipp and Walter 1973; Taniguchi and Suzuki 1983). The development and wide spread of the physical-biophysical methods usable to assay protein structure gave a renaissance to high-pressure protein research. In the meantime several practical applications appeared: pressure treatment of biological systems, like microorganisms and complex food systems were studied and some of these studies led to the development of products which were successfully commercialized (Sasagawa et al. 2005; Yamakura et al. 2005; Rastogi et al. 2007; Yaldagard et al. 2008; Knorr et al. 2011). Simultaneously more and more proteins were experimentally investigated and characterized under pressure as part of basic research projects (Brandts et al. 1970; Hawley 1971; Panick et al. 1999; Smeller et al. 1999; Lassalle et al. 2000; Meersman et al. 2002, 2005; Smeller 2002, 2009; Maeno et al. 2009; Somkuti et al. 2012, 2013a, b).

These achievements on both pure and applied scientific level required the clear thermodynamic description of the underlying processes, among them the description of the protein denaturation under effect of various thermodynamic parameters like pressure and temperature. The first attempt to give a simple but consistent picture was presented by Hawley describing the unfolding  $p$ - $T$  diagram of chymotrypsin (Hawley 1971). He also analyzed the data obtained on ribonuclease-A by Brandts (Brandts et al. 1970). Since then a number of proteins were studied under pressure, and the complete  $p$ - $T$  phase diagrams have been determined for several of them (Zipp and Walter 1973; Panick et al. 1999; Lassalle et al. 2000; Meersman et al. 2005; Smeller 2002; Maeno et al. 2009; Somkuti et al. 2011, 2012, 2013a). This review summarizes the present knowledge about the  $p$ - $T$  phase diagram of protein unfolding.

## 2.2 The Thermodynamic Picture

A typical protein consisting of about 100 residues has several hundred degrees of freedom due to possible rotation around two bonds in each residue. This results in an astronomically high number of possible conformations while generally only few of them are biologically active. Finding these conformations can be described by the folding funnel, which clearly represents the nonrandom, free energy driven nature of the folding process (Fig. 2.1) (Dill and Chan 1977; Bryngelson et al. 1995).

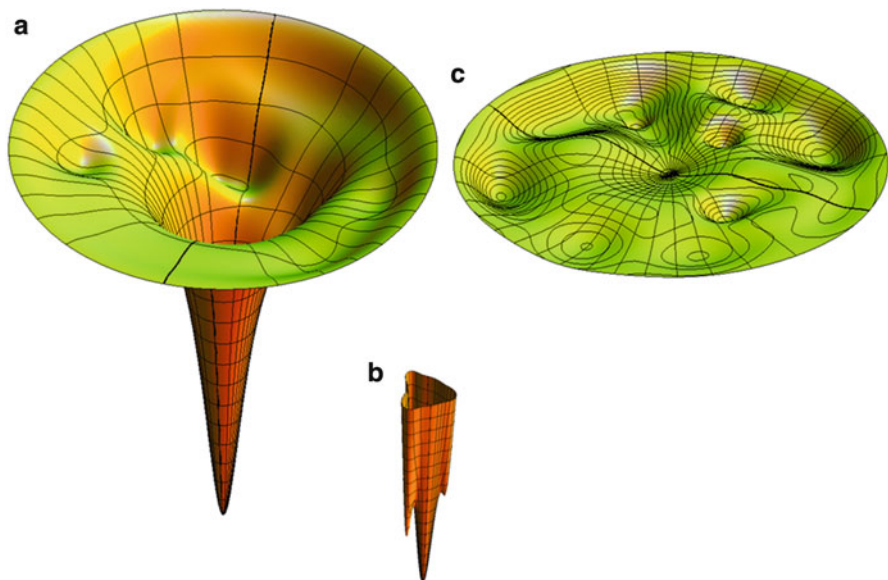


**Fig. 2.1** The folding funnel which explains the directed nature of the folding process. **(a)** under conditions where the native state of the protein is thermodynamically stable, **(b)** the enlarged view of the bottom of the funnel shows several low lying conformations, **(c)** the same energy landscape under denaturing conditions

The protein folding is a complex phenomenon (Osvath et al. 2003, 2009; Gruebele 2009). Although some proteins fold co-translationally or quickly after being synthesized, there are some which face the danger of misfolding, if they are not assisted by chaperone. The folding funnel can have a very rugged surface allowing the accumulation of several long lived intermediate structures. Folding of the so called downhill folder proteins is fast and simple; no partially folded states appear on the folding pathway (Liu and Gruebele 2008). In this case the folding and the unfolding of the protein can be treated as simple two state processes:

$$N \leftrightarrow U$$

where N and U refer to the native and unfolded states respectively.

### 2.2.1 *Thermodynamic Description of the Two State Folding: The Elliptic Phase Diagram*

If we can treat the folding-unfolding process as a simple two-state one, the thermodynamic description is based on the Gibbs free energy difference between the native and unfolded states (Smeller 2002; Hawley 1971):

$$\Delta G = G_U - G_N \quad (2.1)$$

The Gibbs free energies of all states of the protein are pressure and temperature dependent. Treatment of these dependencies can be simplified by a Taylor expansion of the Gibbs free energy. Choosing an appropriate reference point  $(T_0, p_0)$ , and including up to second order terms, we obtain:

$$\begin{aligned}\Delta G = \Delta G_0 &+ \left( \frac{\partial \Delta G}{\partial T} \right)_0 (T - T_0) + \frac{1}{2} \left( \frac{\partial^2 \Delta G}{\partial T^2} \right)_0 (T - T_0)^2 \\ &+ \left( \frac{\partial \Delta G}{\partial p} \right)_0 (p - p_0) + \frac{1}{2} \left( \frac{\partial^2 \Delta G}{\partial p^2} \right)_0 (p - p_0)^2 \\ &+ \left( \frac{\partial^2 \Delta G}{\partial T \partial p} \right)_0 (T - T_0) (p - p_0)\end{aligned}\quad (2.2)$$

where  $\Delta G_0 = \Delta G(T_0, p_0)$ , and all the derivatives have to be calculated at the reference point  $(T_0, p_0)$ . The derivatives of  $\Delta G$  can be written using thermodynamic parameters, like volume ( $V$ ), compression ( $\kappa$ ), entropy ( $S$ ), isobaric heat capacity ( $C_p$ ) and thermal expansivity ( $\alpha$ ), according to the following thermodynamic definitions:

$$\begin{aligned}- \left( \frac{\partial \Delta G}{\partial T} \right)_p &= \Delta S & \left( \frac{\partial \Delta G}{\partial p} \right)_T &= \Delta V \\ - \left( \frac{\partial^2 \Delta G}{\partial T^2} \right)_p &= \frac{\Delta C_p}{T} & - \left( \frac{\partial^2 \Delta G}{\partial p^2} \right)_T &= \Delta \kappa & \left( \frac{\partial^2 \Delta G}{\partial T \partial p} \right) &= \Delta \alpha\end{aligned}\quad (2.3)$$

The free energy difference can be now written as:

$$\begin{aligned}\Delta G = \Delta G_0 &- \Delta S_0 (T - T_0) - \frac{\Delta C_p}{2T_0} (T - T_0)^2 \\ &+ \Delta V_0 (p - p_0) - \frac{\Delta \kappa}{2} (p - p_0)^2 + \Delta \alpha (T - T_0) (p - p_0) + \dots\end{aligned}\quad (2.4)$$

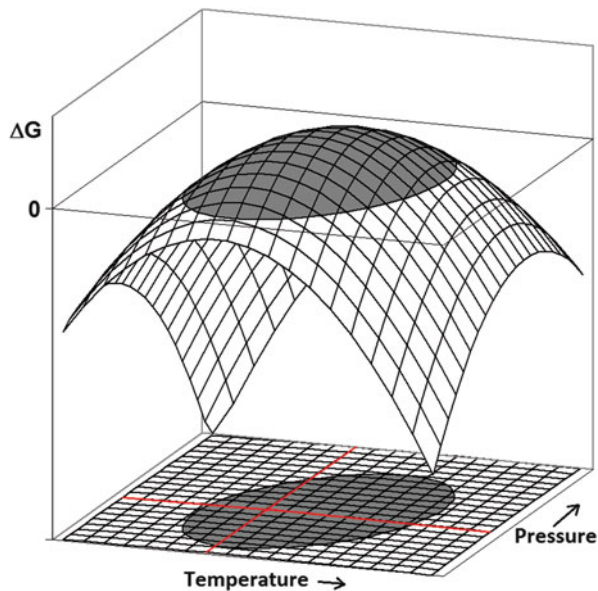
where  $\Delta$  refers to the difference of the value in unfolded and native state (similarly to Eq. 2.1). The subscript 0 indicates that the value has to be taken at the reference point  $(T_0, p_0)$ . The truncation of the series at the second order terms means that we neglect the temperature and pressure dependence of the second order derivatives, i.e.  $C_p$ ,  $\kappa$  and  $\alpha$  are independent of  $T$  and  $p$ . This is why they do not have a zero index.

Compressibility is defined by:

$$\beta = -\frac{1}{V} \left( \frac{\partial V}{\partial p} \right)_T \quad (2.5)$$

It has to be noted, that an expression similar to the right hand side of Eq. 2.4 can be obtained for  $\Delta G$  if one starts to integrate the changes in  $\Delta G$  starting from the

**Fig. 2.2** Gibbs free energy of unfolding as a function of pressure and temperature. The *thick ellipse* indicates the transition curve where  $\Delta G = 0$ . Inside the ellipse the native, outside the unfolded state is stable



$(T_0, p_0)$  point until any arbitrary  $(T, p)$  point. The only difference is in the third term of the right hand side of Eq. 2.4, which is given by:

$$-\Delta C_p \left[ T \left( \ln \frac{T}{T_0} - 1 \right) + T_0 \right] \quad (2.6)$$

This can be approximated by the third term of Eq. 2.4 if  $(T - T_0)/T_0 \ll 1$ .

From mathematical point of view Eq. 2.4 describes a dome-shaped surface as function of  $T$  and  $p$  as shown in Fig. 2.2. The boundary of the native phase can be obtained by:

$$\Delta G(T_i, p_i) = 0 \quad (2.7)$$

where  $(T_i, p_i)$  is an arbitrary point on the boundary. Crossing this transition boundary one can observe unfolding or folding of the protein. Combining Eqs. 2.4 and 2.7 one gets the quadratic equation for a conic section. The curve can be ellipse, hyperbola or parabola, depending on the discriminant of the equation. In the observed cases of proteins, the boundary of the native state was always an ellipse. The requirement for the elliptic shape is:

$$\Delta \alpha^2 - \Delta \kappa \Delta C_p / T_0 < 0 \quad (2.8)$$

Further requirement to have a real (and not imaginary) ellipse is:

$$-Det / (\Delta \kappa + C_p / T_0) < 0 \quad (2.9)$$

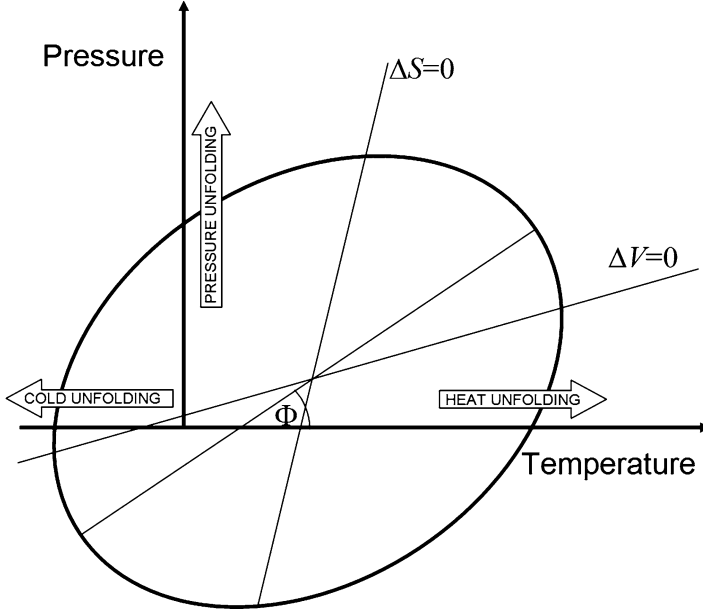


**Fig. 2.3** The elliptic phase diagram

where:

$$Det = \begin{vmatrix} -\frac{\Delta C_p}{2T_0} & \frac{\Delta \alpha}{2} & -\frac{\Delta S_0}{2} \\ \frac{\Delta \alpha}{2} & -\frac{\Delta \kappa}{2} & \frac{\Delta V_0}{2} \\ -\frac{\Delta S_0}{2} & \frac{\Delta V_0}{2} & \Delta G_0 \end{vmatrix}$$

These requirements seem to be fulfilled for the protein solutions studied so far. The experimental transition points can be well fitted with an elliptic curve in a number of published cases (Brandts et al. 1970; Hawley 1971; Panick et al. 1999; Lassalle et al. 2000; Maeno et al. 2009; Somkuti et al. 2013a). If the  $\Delta G(T, p)$  function follows a dome shape, like the one in Fig. 2.2, the elliptic boundary surrounds the region, where the protein is native, while outside of the elliptic region it is unfolded (see Fig. 2.3).

The central point  $(T_c, p_c)$  of the ellipse is given by the solution of the following system of linear equations:

$$\begin{aligned} -\frac{\Delta C_p}{T_0} T_c + \Delta \alpha p_c - \Delta S_0 &= 0 \\ \Delta \alpha T_c - \Delta \kappa p_c + \Delta V_0 &= 0 \end{aligned} \quad (2.10)$$

More interestingly, the angle  $\Phi$  between the temperature axis and the principal axis of the ellipse (Fig. 2.3) is given by the following equation:

$$\operatorname{tg} 2\Phi = -\frac{2\Delta\alpha}{\Delta C_p/T_0 - \Delta\kappa} \quad (2.11)$$

This equation emphasizes the role of the thermal expansivity ( $\Delta\alpha$ ) in the determination of the direction of the ellipse.

The elliptic diagram in Fig. 2.3 makes it clear that the usually observed heat unfolding and also the pressure and the cold unfolding are only three special cases from the infinitely many possibilities to cross the elliptic boundary and unfold the protein. A number of papers tried to explore and compare these three specific unfolding ways. Cold unfolding of proteins was described and its thermodynamics has been analyzed in details by Privalov (1990, 1997). It was however observed only for few proteins, since the cold unfolding temperature often falls below the freezing point of water. This problem was overcome by high pressure experimentalists, by using a subdenaturing pressure, where the freezing point of the water could be lowered by ca. 20 °C (at 200 MPa). This trick is called pressure assisted cold unfolding. Cold denaturations of ribonuclease A (Zhang et al. 1995) myoglobin (Meersman et al. 2002, 2005) and ubiquitin (Kitahara and Akasaka 2003) were measured using this method.

An important question is, whether the unfolded states are different if the unfolding path is different? Are there distinct heat-denatured, pressure denatured and cold denatured states? A clear proof would be if one could observe a phase transition when the cold or pressure denatured protein is heated above the heat denaturation temperature under sufficiently high pressure to keep it in the unfolded state, and subsequently it is cooled to the atmospheric pressure (reaching the heat denaturation conditions) without crossing the elliptic boundary. No such transition was ever detected. This does not necessarily mean the identity of these unfolded states, it indicates that the transition between them is smooth if it exists. We can recall a well-known example from the physical chemistry of water. It is possible to go smoothly from water to vapor (without phase transition) if the path goes above the critical point. Similar smooth conformational drift can also happen within the unfolded ensemble of polypeptide chains in the denatured phase.

From a thermodynamic point of view the driving force in case of the cold, heat and pressure denaturations is different. In Fig. 2.3 the lines for  $\Delta V = 0$  and  $\Delta S = 0$  are also shown. Their position on the phase diagram makes clear that the pressure and cold unfolding are driven mainly by  $\Delta V$  while in case of heat unfolding  $\Delta S$  plays the most important role. This was confirmed by NMR experiments on Ribonuclease A, where the protection factors for the H/D exchange were similar for the cold and the pressure unfolded states. These states were also found to be more compact than the heat unfolded structure (Nash et al. 1996).

The above theory gives a very general description. It does not consider any specific feature of the protein, thus any two-state system which fulfills Eq. 2.8 will

show an elliptic phase diagram. There are examples in the literature of the liquid crystals for similar elliptic phases, which are called there as “re-entrant” phases (Cladis 1988).

### 2.2.2 Limitations of the Simple Thermodynamic Theory

The elliptic shape of the phase diagram is the consequence of the fact that we stopped the series expansion at the second order terms. This means physically, that the coefficients of the second order terms (i.e.  $\Delta C_p$ ,  $-\Delta\kappa$ ,  $\Delta\alpha$ ) are temperature and pressure independent. If this is not true, the third order terms proportional to  $(T - T_0)^3$ ,  $(T - T_0)^2(p - p_0)$ ,  $(T - T_0)(p - p_0)^2$  and  $(p - p_0)^3$  have to be taken into account. Several experimental works found pressure or temperature dependence of the above coefficients, e.g. pressure dependence of  $C_p$  was reported in the case of ribonuclease A (Yamaguchi et al. 1995).

In our earlier work we pointed out that the third order terms do not cause significant alteration from the elliptic shape, if the  $T$  and  $p$  dependencies of  $\Delta C_p$ ,  $-\Delta\kappa$  and  $\Delta\alpha$  are not too large (Smeller 2002; Smeller and Heremans 1997). This could be the reason for the success of the above theory, since the small deviations do not influence the fitting of the experimental values with the elliptic boundary.

Further significant limitation to the use of the elliptic phase diagram could be the existence of intermediate states on the folding pathway. This results in the existence of metastable states: in certain regions of the phase diagram two or even more structures can appear depending on the history of the sample.

Another important issue, which is not taken into account in the above simple theory, is the appearance of the intermolecular interactions in the denatured and/or intermediate states. This can lead to misfolding or to formation of amorphous or fibrous aggregates, depending on the physicochemical environment of the polypeptide chain. The fibrous aggregates are of interest in the medical research, since such insoluble protein aggregates are associated with a number of neurodegenerative diseases, like Alzheimer’s disease, type II diabetes and the transmissible spongiform encephalopathies (Stefani and Dobson 2003; Meersman and Dobson 2006). Amorphous aggregates are however everyday features in the food industry or in the kitchen. The simplest example for this is the heat denaturation, where a majority of the proteins forms amorphous aggregates. It has been shown that the amorphous and the fibrous aggregates have drastically different pressure stability (Dirix et al. 2005). Since aggregation is a slow and multistep process (Smeller et al. 2004, 2006, 2008), its description using methods of the equilibrium thermodynamics is very difficult.

## 2.3 Experimentally Determined Phase Diagrams

The first important step in this field was done by Hawley (1971), who introduced the elliptic phase diagram and experimentally verified his concept on



chymotrypsinogen. He also used the data measured by Brandts (Brandts et al. 1970) on ribonuclease, to support his elliptic theory. Since that a number of pressure-temperature phase diagrams were recorded. Here we discuss some examples, without attempting to be exhaustive.

### 2.3.1 Myoglobin

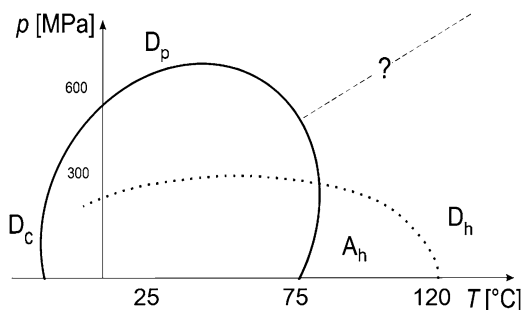
The phase diagram of myoglobin was first studied by Zipp and Kauzmann (Zipp and Kauzmann 1973). They investigated sperm whale metmyoglobin. The boundary of the folded state was represented by curves similar to ellipses. The size of the  $p$ - $T$  region of the native state was strongly dependent on the pH of the solution. Also a remarkable observation is that the experiments were very difficult to perform in the high-temperature and high-pressure region of the phase diagram. Here the system showed long relaxation times and it was very difficult to reach equilibrium. Additionally, in the pH range of 5–9 they reported precipitation of the sample especially at high temperatures.

Zipp and Kauzmann used absorption spectroscopy to detect the phase transitions, where they measured the signal of the prosthetic group namely the absorption of the porphyrin ring, which means the information they obtained reported only indirectly the structure of the polypeptide chain.

Infrared studies on myoglobin were performed in Heremans's laboratory. The amide I band of the infrared spectrum (between 1,600 and 1,700  $\text{cm}^{-1}$ ) is directly characteristic for the secondary structure of the protein (Susi and Byler 1986; Smeller et al. 1995), while the intensity of the amide II band (around 1,550  $\text{cm}^{-1}$ ) shows the hydrogen deuterium exchange and thus it reports the loosening of the tertiary structure.

Meersman et al. used infrared spectroscopy to compare the cold, heat and pressure unfolded states of metmyoglobin from horse heart (Meersman et al. 2002). In a successive work they measured the complete  $p$ - $T$  phase diagram of myoglobin (Meersman et al. 2005). Infrared measurements require high protein concentration, which makes the aggregation of the protein at high temperature and low pressure unavoidable. Since the aggregation is irreversible, the aggregated phase remains stable (or metastable) after returning to ambient conditions. Under these circumstances a purely equilibrium phase diagram cannot be constructed. In certain regions of the  $p$ - $T$  diagram two or even three metastable states can coexist, depending on the history of the sample. Aggregation is disfavored by pressure, therefore aggregation does not happen in pressure denaturation experiments, but folding intermediate states can form during the release of the pressure (Smeller et al. 1999). These intermediates can either refold or aggregate, depending on the temperature. In many cases three states can be observed at ambient conditions: native, aggregated, folding intermediate (Smeller 2002). The high-temperature behavior of the aggregated phase was investigated in detail also by the group of Heremans (Meersman et al. 2005). Interestingly, they found, that the high-temperature aggregates can be

**Fig. 2.4** Phase diagram of myoglobin (Reprinted with permission from Meersman et al. (2005), Copyright 2005 John Wiley and Sons)



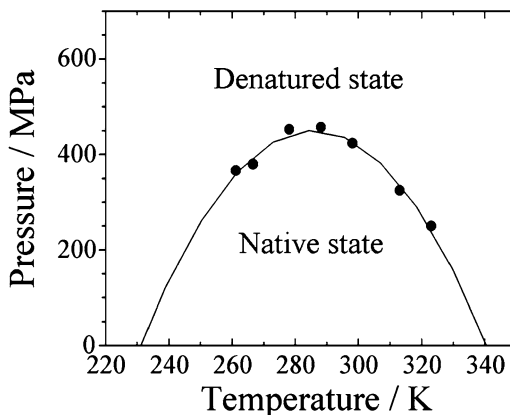
dissociated not only by pressure as it was thought before, but they also dissociate at very high temperatures, well above 100 °C. Similar results were obtained for lysozyme under reducing conditions (Meersman and Heremans 2003). The hypothesis emerged that a similar elliptic phase boundary could be constructed for the aggregated phase, as it is known for the native one (Meersman et al. 2005) (Fig. 2.4). This hypothesis has never been tested experimentally in detail, although it seems quite plausible. The difficulties lie again in the very slow kinetics of the aggregation.

### 2.3.2 Lysozyme

A number of experimental works were published on the pressure and temperature unfolding of lysozyme (Sasahara et al. 2001; Refaee et al. 2003; Vogtt and Winter 2005; Maeno et al. 2009; Smeller 2009). Most often the hen egg white (HEW) lysozyme was investigated, since it is commercially available. Lysozyme is quite pressure stable under neutral pH, the midpoint of the pressure unfolding is 680 MPa at 25 °C (Smeller et al. 2006).

Akasaka's group determined the detailed phase diagram of HEW lysozyme at pH 2 using  $^1\text{H}$ -NMR and Trp fluorescence spectroscopies (Maeno et al. 2009). Figure 2.5 shows the pressure-temperature diagram obtained by them. As it is clear from the figure, lowering the pH reduces pressure stability to 450 MPa, which was obtained at 5 °C. They analyzed their data using a similar thermodynamic analysis to the one described in Eq. 2.4. They neglected, however, the difference of the compressibility between the native and unfolded state based on an earlier work (Royer 2006). This assumption makes the elliptic barrier similar to a parabolic one, which describes the experimental points in this case quite well. The maximum position of the fluorescence emission was fitted by a sigmoid curve, which describes the two-state transition. The NMR results followed the same model quite well in the pressure range, where NMR spectroscopy was available. Lysozyme denaturation at low pH was shown in this paper to behave as a two-state process in the whole pressure-temperature region studied (Maeno et al. 2009).

**Fig. 2.5** Phase diagram of lysozyme at pH 2 (Reprinted from BIOPHYSICS Vol. 5 (pp. 1–9, 2009) (Maeno et al. 2009), with permission)



FTIR spectroscopic experiments were performed by Heremans's group at neutral pH (Smeller et al. 2006). They suggested the presence of folding intermediates, which can be considerably populated on the refolding path, similarly to the case of myoglobin mentioned above (Smeller 2002). Our later experiments showed the existence of molten globule states in the pressure-temperature phase diagram of lysozyme. The formation of molten globule precedes the temperature and also the pressure unfolding (Smeller 2009). Deviation from the two-state unfolding was found in complex environment, where the effect of mild ( $\leq 100$  MPa) pressure on denaturant (GdnCl) induced unfolding of lysozyme at pH 4 was investigated (Sasahara et al. 2001).

Winter's group studied the heat denatured and the pressure assisted cold denatured state of HEW lysozyme using COSY proton NMR (Vogt and Winter 2005). They measured the hydrogen-deuterium exchange rate and determined the protection factors for several amino acid residues. The exchange kinetics upon heat treatment was found to be a two-step process with an initial slow exchange followed by a fast one. This was interpreted by the protection of the slow exchanging transient state. Such effect was not found at cold denaturation.

Since lysozyme is quite stable its pressure region, which causes no unfolding, but only elastic deformations, is broad and can be conveniently studied (Refaee et al. 2003). The effect of subdenaturing pressure gives valuable information about the structure of the folding energy landscape. Pressure stabilizes selectively the conformations with smaller volumes. These conformational states are present under physiological conditions, but they cannot be observed due to their low thermodynamic probability in ambient conditions. Subdenaturing pressures can reveal these conformations (Akasaka et al. 2013).

Besides HEW lysozyme, the T4 lysozyme was also investigated extensively. A number of mutants were prepared in Matthews's laboratory with cavities of different size inside the protein (Ando et al. 2008). The cavity formation influenced the volume change ( $\Delta V$ ) and the unfolding pressure too. The main conclusion from the

pressure unfolding studies on the cavity forming mutants was that water penetration into the protein interior is more consistent with the results, rather than transfer of the hydrophobic residues to the water during the pressure denaturation (Ando et al. 2008).

### 2.3.3 Ribonuclease

Ribonuclease A is one of the first proteins whose phase diagram was determined (Brandts et al. 1970; Hawley 1971). Since that, many pressure experiments were performed on different types of ribonucleases (Yamaguchi et al. 1995; Nash et al. 1996; Yamasaki et al. 1998; Ribo et al. 2006; Zhai and Winter 2013). Jonas's group compared the cold, heat and pressure denaturation of ribonuclease using NMR spectroscopy (Zhang et al. 1995).

Recently the phase diagram of ribonuclease A was reinvestigated to study the effect of molecular crowding on the phase diagram (Zhai and Winter 2013). Dextran was used as crowding. Molecular crowding caused by 30 % dextran stabilized the folded state of the protein against both pressure and heat denaturation (Fig. 2.6) (Zhai and Winter 2013). Understanding the effect of molecular crowding is important, since the cellular environment is highly crowded.

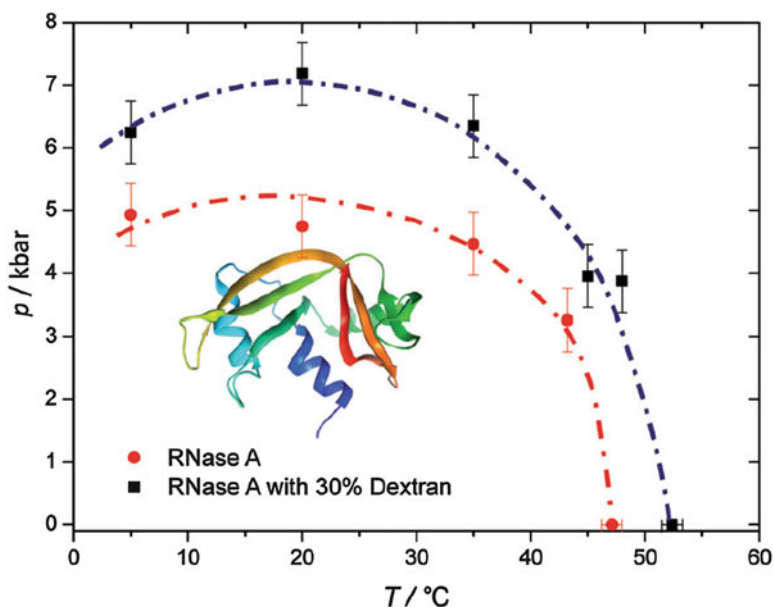


**Fig. 2.6** Phase diagram of Ribonuclease A with and without crowding agent (dextran) (Reprinted with permission from Zhai and Winter (2013), Copyright 2013 John Wiley and Sons)

### 2.3.4 *Staphylococcal Nuclease (SNase)*

Staphylococcal nuclease is a small 17.5 kDa protein containing 149 residues and no disulfide bonds. According to the crystal structure roughly one quarter of the structure is helical and another quarter of the residues belong to beta structure (Hynes and Fox 1991). It has a relatively large number of ionizable side groups. SNase has one single tryptophan residue, which makes it ideal for fluorescence studies. A number of high pressure works were performed on SNase and on its mutants, to explore its pressure behavior and to describe the role of hydration and cavities in the pressure unfolding, and to study the effect of different cosolvents (Stites et al. 1991; Frye and Royer 1998; Panick et al. 1999; Herberhold et al. 2004; Kitahara et al. 2011; Roche et al. 2012; Zhai and Winter 2013).

The pressure-temperature phase diagram of SNase was determined by the groups of Winter, Royer and Akasaka, using several experimental techniques, like tryptophan fluorescence, FTIR spectroscopy, small-angle X-ray scattering (Panick et al. 1999) and NMR spectroscopy (Lassalle et al. 2000). The results allowed to create the  $p$ - $T$  phase diagram of the protein at pH 5.5 (Fig. 2.7). The phase boundary resembles the elliptic shape, although fitting to the Eq. 2.4 was not done. The tryptophan fluorescence experiments gave slightly lower denaturation pressures, which can probably be explained by the terminal position of the tryptophan residue. The V66A mutant (Stites et al. 1991) was also investigated, and both the pressure and the temperature stability of the mutant was found smaller than those of the wild type.

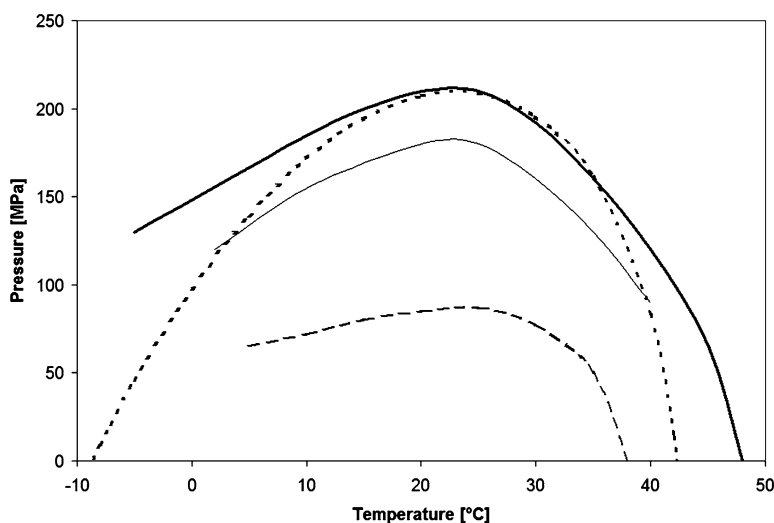


**Fig. 2.7** Phase diagram of SNase (Adapted with permission from (Panick et al. 1999), Copyright 1999 American Chemical Society). *Thick line*: wild type SNase measured by FTIR and SAXS; *thin line*: wild type measured by fluorescence; *broken line*: V66A SNase by FTIR. The *dotted curve* was calculated from the parameters in Lassalle et al. (2000)

**Table 2.1** Fitted parameters of Eq. 2.4

Parameter	Unit	Chimotrypsinogen <sup>a</sup>	Ribonuclease <sup>a</sup>	Snase <sup>b</sup>
$\Delta G_0$	$\text{kJ mol}^{-1}$	10.6	10.5	13.18
$\Delta S_0$	$\text{kJ (mol} \cdot \text{K)}^{-1}$	-0.95	0.052	0.32
$\Delta V_0$	$\text{ml mol}^{-1}$	-14.3	-48.6	-41.9
$\Delta C_p$	$\text{kJ (mol} \cdot \text{K)}^{-1}$	15.9	7.11	13.12
$\Delta \kappa$	$\text{ml (MPa} \cdot \text{mol)}^{-1}$	0.296	0.195	0.2
$\Delta \alpha$	$\text{ml (mol} \cdot \text{K)}^{-1}$	1.32	0.252	1.33
$T_0$	$^{\circ}\text{C}$	0	0	24
$p_0$	MPa	0.1	0.1	0.1
pH		2.07	2.0	5.3

<sup>a</sup>From Hawley (1971)<sup>b</sup>From Lassalle et al. (2000)

Akasaka's group determined the parameters of the Eq. 2.4 from a series of pressure experiments at different temperatures. They obtained the unfolding curves of Snase by following the  $\varepsilon$  protons of His8 and His124 (Lassalle et al. 2000). The parameters obtained for the elliptic fit are listed in the Table 2.1. The ellipse constructed from their parameters is also drawn in Fig. 2.7.

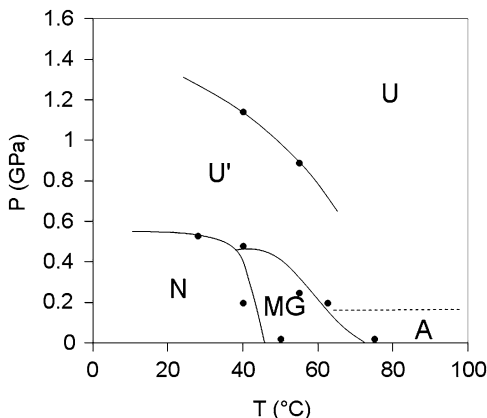
Several mutants of Snase were expressed and characterized. The most interesting of them were the mutations in which residue 66 was exchanged. This residue is buried in the hydrophobic core. The V66K mutation was found to affect the plasticity and stability of the protein (Kitahara et al. 2011).

Another important branch of investigations focused on the effect of chaotropic and cosmotropic cosolvents on the pressure and temperature stability. While glycerol, sorbitol, sucrose and  $\text{K}_2\text{SO}_4$ , increased the stability against pressure unfolding,  $\text{CaCl}_2$  and urea destabilized the protein. The pressure stabilization and the temperature stabilization effects correlated well with each other (Herberhold et al. 2004).

### 2.3.5 The Rv3221c Protein from *Mycobacterium Tuberculosis*

The Rv3221c protein can be found in *Mycobacterium tuberculosis* (Cole et al. 1998). Its specific function is not clear yet, but its importance can be hypothesized from the fact that this protein is highly conserved in *Mycobacteria* (Cole et al. 2001; Kumar et al. 2008). In our experiments the protein showed mainly beta structure, which unfolded at both high temperature and high pressure giving a  $p$ - $T$  diagram with a nice elliptic shape (Somkuti et al. 2013a). The midpoint of the pressure unfolding was 530 MPa (at 30  $^{\circ}\text{C}$ ), while the heat unfolding happened at 65  $^{\circ}\text{C}$  (around atmospheric pressure). The native state binds biotin, which presumably stabilizes the native conformation. Biotin dissociates in the pressure-unfolded state, and only part of the polypeptide chains rebind biotin after the release of the pressure.

**Fig. 2.8** Phase diagram of cod parvalbumin (Gad m1.01) (Reprinted with permission from Somkuti et al. (2012), Copyright 2012 American Chemical Society)



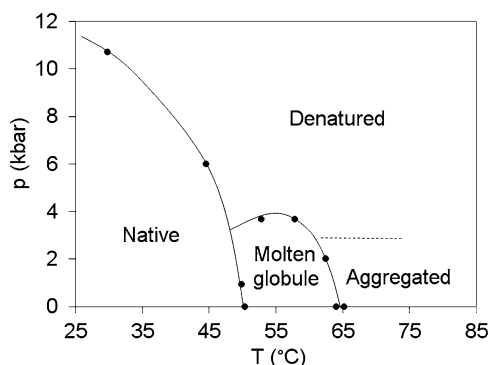
### 2.3.6 Parvalbumin

We have chosen parvalbumin for our  $p$ - $T$  studies, because it is the main allergen protein in fish (Ma et al. 2008). Exploration of the phase diagram of allergen proteins can provide information about possible pressure inactivation (Somkuti and Smeller 2013). Parvalbumin is a small protein consisting of 109 residues. It has a mostly helical structure. The helices form so called EF-hand motives, which can accommodate two  $\text{Ca}^{2+}$ -binding sites. Usually the presence of  $\text{Ca}^{2+}$  ions makes the unfolding far more complex than a two state process. The phase diagram of cod parvalbumin is also quite exotic (Fig. 2.8) (Somkuti et al. 2012). Although the overall elliptic shape can be recognized on the diagram, a number of states appear besides the usual folded and unfolded states. The protein adopts a molten globule state at temperatures above 50 °C at ambient pressure. This structure unfolds and immediately aggregates if the temperature reaches 75 °C. Pressure unfolding also shows two steps. A residual structure remains in the partially unfolded state above 500 MPa. Very high pressure and elevated temperature is needed to reach the completely unfolded state. This phase diagram is a remarkable example for the complexity of the unfolding process, and for the appearance of the folding intermediates, if additional stabilizing factors are present, like the two  $\text{Ca}^{2+}$ -binding sites of parvalbumin.

### 2.3.7 IG27 of Titin

Titin is the largest protein in nature, with a molar weight exceeding 3 MDa (Labeit et al. 1990). It is responsible for the passive force generated upon stretching the muscle (Trombitas et al. 1998). Titin structure is dominated by two structurally different types of elements. Over 90 % of its molecular weight is made up of immunoglobulin

**Fig. 2.9** Phase diagram of I27 domain of titin (Reprinted with permission from Somkuti et al. (2013b), Copyright 2013 Elsevier)



and fibronectin III domains. The remaining 10 % is a disordered segment (called PEVK domain) (Labeit et al. 1990; Labeit and Kolmerer 1995). The most studied immunoglobulin domain is the I27, which has a beta sandwich fold and contains a single tryptophan residue in the middle, making it ideal for the folding studies by both FTIR and fluorescence spectroscopy. The pressure-temperature phase diagram of I27 was determined using FTIR and tryptophan fluorescence spectroscopies in our laboratory (Fig. 2.9) (Somkuti et al. 2013b). The most remarkable feature of the diagram is the appearance of the molten globule state at slightly elevated temperature in the low-pressure region. The native  $\rightarrow$  molten globule transition could be clearly detected by tryptophan fluorescence. At 50 °C the compact structure of the protein opens, and the polarity of the interior changes. Simultaneously the infrared spectrum shows the completion of the hydrogen-deuterium exchange, showing the loosening of the tertiary structure. The secondary structure, however, disappears only above 65 °C, where the protein aggregates immediately after the unfolding.

The pressure unfolding was found to be a two-state transition, without formation of any intermediates or partially folded states.

### 2.3.8 Intrinsically Disordered Proteins (IDPs)

Recently a big family of IDPs has been described, which do not follow the classical structure–function paradigm (Tompa 2009). They show a disordered conformation under physiological conditions. Different types of IDPs exist: some will be ordered upon binding to their target proteins, but a distinct category of them acts as entropic spring. The PEVK domain of titin is a typical example for such proteins.

From thermodynamic point of view it is an important question, whether the elliptic folded phase of these proteins is just shifted far from the physiological conditions on the  $p$ - $T$  diagram, or it is completely absent. The latter case means that  $\Delta G$  is always negative, for all ( $p, T$ ) points of the pressure-temperature phase diagram, i.e. the inequality of Eq. 2.9 is not fulfilled. Visually this means that the whole dome-shaped curve of Fig. 2.2 is under the zero level of  $\Delta G$ .



This area is mainly uncovered yet, since pressure works on IDPs are practically absent from the literature. The PEVK domain of titin was investigated by FTIR spectroscopy under various pH and temperature conditions (Somkuti et al. 2013b). Since these experiments did not reveal any region where the polypeptide chain would adopt any ordered structure, the second situation discussed above is more probable for PEVK, which means that this protein domain has always negative  $\Delta G$ .

## 2.4 Concluding Remarks

The conventional Hawley theory leads to an elliptic boundary in the pressure-temperature plane for the native state. The theory is based on a two-state assumption. It can treat only situations in which only the native and the unfolded states are populated significantly. The model can describe a number of simple proteins in a dilute solution. This model fails to take into account the intermolecular interactions, and the consequent aggregation processes. If molten globule or partially folded intermediates can appear in certain ranges of the pressure-temperature plane, the phase diagram can be more complex. The complexity of the phase diagram becomes particularly apparent, if there are several factors which stabilize the protein, e.g. when binding of ions plays stabilizing role.

Since proteins in their native environment are tightly surrounded by other macromolecules, intermolecular interactions, and their effect on the native state, and also their effect on the phase diagram are of particular interest.

**Acknowledgement** This work was supported by the Hungarian Research Fund project OTKA 77730. The author is very grateful to Sz. Osvath for reading the manuscript and for the fruitful discussions.

## References

- Akasaka K, Kitahara R, Kamatari YO (2013) Exploring the folding energy landscape with pressure. *Arch Biochem Biophys* 53:110–115. doi:[10.1016/j.abb.2012.11.016](https://doi.org/10.1016/j.abb.2012.11.016)
- Ando N, Barstow B, Baase WA, Fields A, Matthews BW, Gruner SM (2008) Structural and thermodynamic characterization of T4 lysozyme mutants and the contribution of internal cavities to pressure denaturation. *Biochemistry* 47:11097–11109. doi:[10.1021/bi801287m](https://doi.org/10.1021/bi801287m)
- Brandts JF, Oliveira RJ, Westort C (1970) Thermodynamics of protein denaturation. Effect of pressure on the denaturation of ribonuclease A. *Biochemistry* 17:1038–1047
- Bridgman PW (1914) The coagulation of albumen by pressure. *J Biol Chem* 19:511–512
- Bryngelson JD, Onuchic JN, Socci ND, Wolynes PG (1995) Funnels, pathways, and the energy landscape of protein folding: a synthesis. *Proteins Struct Funct Genet* 21:167–195. doi:[10.1002/prot.340210302](https://doi.org/10.1002/prot.340210302)
- Cladis PE (1988) A 100 year perspective of the reentrant nematic phase. *Mol Cryst Liq Cryst* 165:85–121. doi:[10.1080/00268948808082197](https://doi.org/10.1080/00268948808082197)

- Cole ST, Brosch R, Parkhill J, Garnier T, Churcher C, Harris D, Gordon SV, Eiglmeier K, Gas S, Barry CE, Tekaia F, Badcock K, Basham D, Brown D, Chillingworth T, Connor R, Davies R, Devlin K, Feltwell T, Gentles S, Hamlin N, Holroyd S, Hornby T, Jagels K, Krogh A, McLean J, Moule S, Murphy L, Oliver K, Osborne J, Quail MA, Rajandream MA, Rogers J, Rutter S, Seeger K, Skelton J, Squares R, Squares S, Sulston JE, Taylor K, Whitehead S, Barrell BG (1998) Deciphering the biology of *Mycobacterium tuberculosis* from the complete genome sequence. *Nature* 393(6685):537–544
- Cole ST, Eiglmeier K, Parkhill J, James KD, Thomson NR, Wheeler PR, Honore N, Garnier T, Churcher C, Harris D, Mungall K, Basham D, Brown D, Chillingworth T, Connor R, Davies RM, Devlin K, Duthoy S, Feltwell T, Fraser A, Hamlin N, Holroyd S, Hornsby T, Jagels K, Lacroix C, Maclean J, Moule S, Murphy L, Oliver K, Quail MA, Rajandream MA, Rutherford KM, Rutter S, Seeger K, Simon S, Simmonds M, Skelton J, Squares R, Squares S, Stevens K, Taylor K, Whitehead S, Woodward JR, Barrell BG (2001) Massive gene decay in the leprosy bacillus. *Nature* 409(6823):1007–1011. doi:[10.1038/35059006](https://doi.org/10.1038/35059006)
- Dill KA, Chan HS (1977) From Levinthal to pathways to funnels. *Nature Struct Biol* 4:10–19
- Dirix C, Meersman F, MacPhee CE, Dobson CM, Heremans K (2005) High hydrostatic pressure dissociates early aggregates of TTR105–115, but not the mature amyloid fibrils. *J Mol Biol* 347:903–909. doi:[10.1016/j.jmb.2005.01.073](https://doi.org/10.1016/j.jmb.2005.01.073)
- Frye KJ, Royer CA (1998) Probing the contribution of internal cavities to the volume change of protein unfolding under pressure. *Protein Sci* 7:2217–2222
- Gruebele M (2009) Protein dynamics: from molecules, to interactions, to biology. *Int J Mol Sci* 10:1360–1368. doi:[10.3390/ijms10031360](https://doi.org/10.3390/ijms10031360)
- Hawley SA (1971) Reversible pressure-temperature denaturation of chymotrypsinogen. *Biochemistry* 10:2436–2442. doi:[10.1021/bi00789a002](https://doi.org/10.1021/bi00789a002)
- Herberhold H, Royer CA, Winter R (2004) Effects of chaotropic and kosmotropic cosolvents on the pressure-induced unfolding and denaturation of proteins: an FT-IR study on staphylococcal nuclease. *Biochemistry* 43:3336–3345. doi:[10.1021/bi036106z](https://doi.org/10.1021/bi036106z)
- Hynes TR, Fox RO (1991) The crystal structure of staphylococcal nuclease refined at 1.7 Å resolution. *Proteins* 10:92–105. doi:[10.1002/prot.340100203](https://doi.org/10.1002/prot.340100203)
- Kitahara R, Akasaka K (2003) Close identity of a pressure-stabilized intermediate with a kinetic intermediate in protein folding. *Proc Natl Acad Sci U S A* 100:3167–3172. doi:[10.1073/pnas.0630309100](https://doi.org/10.1073/pnas.0630309100)
- Kitahara R, Hata K, Maeno A, Akasaka K, Chimenti MS, Garcia-Moreno B, Schroer MA, Jeworrek C, Tolan M, Winter R, Roche J, Roumestand C, de Guillen KM, Royer CA (2011) Structural plasticity of staphylococcal nuclease probed by perturbation with pressure and pH. *Proteins* 79:1293–1305. doi:[10.1002/prot.22966](https://doi.org/10.1002/prot.22966)
- Knorr D, Froehling A, Jaeger H, Reineke K, Schlueter O, Schoessler K (2011) Emerging technologies in food processing. *Ann Rev Food Sci Technol* 2:203–235
- Kumar N, Shukla S, Kumar S, Suryawanshi A, Chaudhry U, Ramachandran S, Maiti S (2008) Intrinsically disordered protein from a pathogenic mesophile *Mycobacterium tuberculosis* adopts structured conformation at high temperature. *Proteins* 71:1123–1133. doi:[10.1002/prot.21798](https://doi.org/10.1002/prot.21798)
- Labeit S, Kolmerer B (1995) Titins – giant proteins in charge of muscle ultrastructure and elasticity. *Science* 270:293–296. doi:[10.1126/science.270.5234.293](https://doi.org/10.1126/science.270.5234.293)
- Labeit S, Barlow DP, Gautel M, Gibson T, Holt J, Hsieh CL, Francke U, Leonard K, Wardale J, Whiting A, Trinick J (1990) A regular pattern of 2 types of 100-residue motif in the sequence of titin. *Nature* 345:273–276. doi:[10.1038/345273a0](https://doi.org/10.1038/345273a0)
- Lassalle MW, Yamada H, Akasaka K (2000) The pressure-temperature free energy-landscape of staphylococcal nuclease monitored by H-1 NMR. *J Mol Biol* 298:293–302. doi:[10.1006/jmbi.2000.3659](https://doi.org/10.1006/jmbi.2000.3659)
- Liu F, Gruebele M (2008) Downhill dynamics and the molecular rate of protein folding. *Chem Phys Lett* 461:1–8. doi:[10.1016/j.cplett.2008.04.075](https://doi.org/10.1016/j.cplett.2008.04.075)

- Ma Y, Griesmeier U, Susani M, Radauer C, Briza P, Erler A, Bublin M, Alessandri S, Himly M, Vazquez-Cortes S, de Arellano IRR, Vassilopoulou E, Saxoni-Papageorgiou P, Knulst AC, Fernandez-Rivas M, Hoffmann-Sommergruber K, Breiteneder H (2008) Comparison of natural and recombinant forms of the major fish allergen parvalbumin from cod and carp. *Mol Nutr Food Res* 52:S196–S207. doi:[10.1002/mnfr.200700284](https://doi.org/10.1002/mnfr.200700284)
- Maeno A, Matsuuo H, Akasaka K (2009) The pressure-temperature phase diagram of hen lysozyme at low pH. *Biophys J* 96:1–9. doi:[10.2142/biophysics.5.1](https://doi.org/10.2142/biophysics.5.1)
- Meersman F, Dobson CM (2006) Probing the pressure-temperature stability of amyloid fibrils provides new insights into their molecular properties. *Biochim Biophys Acta* 1764:452–460. doi:[10.1016/j.bbapap.2005.10.021](https://doi.org/10.1016/j.bbapap.2005.10.021)
- Meersman F, Heremans K (2003) Temperature-induced dissociation of protein aggregates: accessing the denatured state. *Biochemistry* 42:14234–14241. doi:[10.1021/bi035623e](https://doi.org/10.1021/bi035623e)
- Meersman F, Smeller L, Heremans K (2002) Comparative Fourier transform infrared spectroscopy study of cold-, pressure-, and heat-induced unfolding and aggregation of myoglobin. *Biophys J* 82:2635–2644
- Meersman F, Smeller L, Heremans K (2005) Extending the pressure-temperature state diagram of myoglobin. *Helv Chim Acta* 88:546–556
- Nash D, Lee BS, Jonas J (1996) Hydrogen-exchange kinetics in the cold denatured state of ribonuclease A. *Biochim Biophys Acta* 1297:40–48. doi:[10.1016/0167-4838\(96\)00085-4](https://doi.org/10.1016/0167-4838(96)00085-4)
- Osvath S, Sabelko JJ, Gruebele M (2003) Tuning the heterogeneous early folding dynamics of phosphoglycerate kinase. *J Mol Biol* 333:187–199. doi:[10.1016/j.jmb.2003.08.011](https://doi.org/10.1016/j.jmb.2003.08.011)
- Osvath S, Quynh LM, Smeller L (2009) Thermodynamics and kinetics of the pressure unfolding of phosphoglycerate kinase. *Biochemistry* 48:10146–10150. doi:[10.1021/bi900922f](https://doi.org/10.1021/bi900922f)
- Panick G, Vidugiris GJA, Malessa R, Rapp G, Winter R, Royer CA (1999) Exploring the temperature-pressure phase diagram of staphylococcal nuclease. *Biochemistry* 38:4157–4164
- Privalov PL (1990) Cold denaturation of proteins. *Biophys J* 57:A26
- Privalov PL (1997) Thermodynamics of protein folding. *J Chem Thermodyn* 29:447–474. doi:[10.1006/jcht.1996.0178](https://doi.org/10.1006/jcht.1996.0178)
- Rastogi NK, Raghavarao KSMS, Balasubramaniam VM, Niranjana K, Knorr D (2007) Opportunities and challenges in high pressure processing of foods. *Crit Rev Food Sci Nutr* 47:69–112. doi:[10.1080/10408390600626420](https://doi.org/10.1080/10408390600626420)
- Refaee M, Tezuka T, Akasaka K, Williamson MP (2003) Pressure-dependent changes in the solution structure of hen egg-white lysozyme. *J Mol Biol* 327:857–865. doi:[10.1016/s0022-2836\(03\)00209-2](https://doi.org/10.1016/s0022-2836(03)00209-2)
- Ribo M, Font J, Benito A, Torrent J, Lange R, Vilanova M (2006) Pressure as a tool to study protein-unfolding/refolding processes: the case of ribonuclease A. *Biochim Biophys Acta* 1764:461–469. doi:[10.1016/j.bbapap.2005.11.011](https://doi.org/10.1016/j.bbapap.2005.11.011)
- Roche J, Dellarole M, Caro JA, Guca E, Norberto DR, Yang Y, Garcia AE, Roumestand C, Garcia-Moreno B, Royer CA (2012) Remodeling of the folding free energy landscape of staphylococcal nuclease by cavity-creating mutations. *Biochemistry* 51:9535–9546. doi:[10.1021/bi301071z](https://doi.org/10.1021/bi301071z)
- Royer CA (2006) Probing protein folding and conformational transitions with fluorescence. *Chem Rev* 106:1769–1784. doi:[10.1021/cr0404390](https://doi.org/10.1021/cr0404390)
- Sasagawa A, Gomi M, Ohura K, Yamazaki A, Yamada A (2005) Production of Miso based on Koji prepared from mixed different grains using high-pressure treatment. *J Japanese Soc Food Sci Technol-Nippon Shokuhin Kagaku Kogaku Kaishi* 52:485–490
- Sasahara K, Sakurai M, Nitta K (2001) Pressure effect on denaturant-induced unfolding of hen egg white lysozyme. *Proteins- Struct Funct Genet* 44:180–187. doi:[10.1002/Prot.1083](https://doi.org/10.1002/Prot.1083)
- Smeller L (2002) Pressure-temperature phase diagrams of biomolecules. *Biochim Biophys Acta* 1595:11–29
- Smeller L (2009) Evidence for metastable states of lysozyme revealed by high pressure FTIR spectroscopy. *Biophys J* 96:388a. doi:[http://dx.doi.org/10.1016/j.bpj.2008.12.2900](https://doi.org/http://dx.doi.org/10.1016/j.bpj.2008.12.2900)

- Smeller L, Heremans K (1997) Some thermodynamic and kinetic consequences of the phase diagram of protein denaturation. In: Heremans K (ed) High pressure research in bioscience and biotechnology. Leuven University Press, Leuven, pp 55–58
- Smeller L, Goossens K, Heremans K (1995) Determination of the secondary structure of proteins at high pressure. *Vib Spectrosc* 8:199–203
- Smeller L, Rubens P, Heremans K (1999) Pressure effect on the temperature-induced unfolding and tendency to aggregate of myoglobin. *Biochemistry* 38:3816–3820
- Smeller L, Fidy J, Heremans K (2004) Protein folding, unfolding and aggregation. Pressure induced intermediate states on the refolding pathway of horseradish peroxidase. *J Phys* 16:S1053–S1058
- Smeller L, Meersman F, Heremans K (2006) Refolding studies using pressure: the folding landscape of lysozyme in the pressure-temperature plane. *Biochim Biophys Acta* 1764:497–505. doi:[10.1016/j.bbapap.2006.01.016](https://doi.org/10.1016/j.bbapap.2006.01.016)
- Smeller L, Meersman F, Heremans K (2008) Stable misfolded states of human serum albumin revealed by high-pressure infrared spectroscopic studies. *Eur Biophys J* 37:1127–1132
- Somkuti J, Smeller L (2013) High pressure effects on allergen food proteins. *Biophys Chem* 183:19–29. doi:[10.1016/j.bpc.2013.06.009](https://doi.org/10.1016/j.bpc.2013.06.009)
- Somkuti J, Houska M, Smeller L (2011) Pressure and temperature stability of the main apple allergen Mal d1. *Eur Biophys J* 40:143–151. doi:[10.1007/s00249-010-0633-8](https://doi.org/10.1007/s00249-010-0633-8)
- Somkuti J, Bublin M, Breiteneder H, Smeller L (2012) Pressure-temperature stability,  $\text{Ca}^{2+}$  binding, and pressure-temperature phase diagram of cod parvalbumin: Gad m 1. *Biochemistry* 51:5903–5911. doi:[dx.doi.org/10.1021/bi300403h](https://doi.org/10.1021/bi300403h)
- Somkuti J, Jain S, Ramachandran S, Smeller L (2013a) Folding-unfolding transitions of Rv3221c on the pressure-temperature plane. *High Pressure Res* 33:250–257. doi:[10.1080/08957959.2013.780055](https://doi.org/10.1080/08957959.2013.780055)
- Somkuti J, Martonfalvi Z, Kellermayer MSZ, Smeller L (2013b) Different pressure-temperature behavior of the structured and unstructured regions of titin. *Biochim Biophys Acta* 1834:112–118. doi:[10.1016/j.bbapap.2012.10.001](https://doi.org/10.1016/j.bbapap.2012.10.001)
- Stefani M, Dobson CM (2003) Protein aggregation and aggregate toxicity: new insights into protein folding, misfolding diseases and biological evolution. *J Mol Med* 81:678–699. doi:[10.1007/s00109-003-0464-5](https://doi.org/10.1007/s00109-003-0464-5)
- Stites WE, Gittis AG, Lattman EE, Shortle D (1991) In a staphylococcal nuclease mutant the side-chain of a lysine replacing valine-66 is fully buried in the hydrophobic core. *J Mol Biol* 221:7–14. doi:[10.1016/0022-2836\(91\)80195-z](https://doi.org/10.1016/0022-2836(91)80195-z)
- Susi H, Byler DM (1986) Resolution-enhanced Fourier-transform infrared-spectroscopy of enzymes. *Methods Enzymol* 130:290–311
- Suzuki K (1960) Studies on the kinetics of protein denaturation under high pressure. *Rev Phys Chem Jpn* 29:91–98
- Taniguchi Y, Suzuki K (1983) Studies of polymer effects under pressure. Part 7. Pressure inactivation of alpha-chymotrypsin. *J Phys Chem* 87:5185–5193. doi:[10.1021/J150643a025](https://doi.org/10.1021/J150643a025)
- Tompa P (2009) Structure and function of intrinsically disordered proteins. Chapman and Hall/CRC, Boca Raton
- Trombitas K, Greaser M, Labeit S, Jin JP, Kellermayer M, Helmes M, Granzier H (1998) Titin extensibility in situ: entropic elasticity of permanently folded and permanently unfolded molecular segments. *J Cell Biol* 140:853–859. doi:[10.1083/jcb.140.4.853](https://doi.org/10.1083/jcb.140.4.853)
- Vogt K, Winter R (2005) Pressure-assisted cold denaturation of hen egg white lysozyme: the influence of co-solvents probed by hydrogen exchange nuclear magnetic resonance. *Brazilian J Med Biol Res* 38:1185–1193. doi:[10.1590/s0100-879x2005000800005](https://doi.org/10.1590/s0100-879x2005000800005)
- Yaldagard M, Mortazavi SA, Tabatabaie F (2008) The principles of ultra high pressure technology and its application in food processing/preservation: a review of microbiological and quality aspects. *Afr J Biotechnol* 7:2739–2767
- Yamaguchi T, Yamada H, Akasaka K (1995) Thermodynamics of unfolding of ribonuclease A under high pressure. A study by proton NMR. *J Mol Biol* 250:689–694. doi:[10.1006/jmbi.1995.0408](https://doi.org/10.1006/jmbi.1995.0408)

- Yamakura M, Haraguchi K, Okadome H, Suzuki K, Tran UT, Horigane KA, Yoshida M, Homma S, Sasagawa A, Yamazaki A, Ohtsubo K (2005) Effects of soaking and high-pressure treatment on the qualities of cooked rice. *J Appl Glycosci* 52:85–93
- Yamasaki K, Taniguchi Y, Takeda N, Nakano K, Yamasaki T, Kanaya S, Oobatake M (1998) Pressure-denatured state of *Escherichia coli* ribonuclease HI as monitored by Fourier transform infrared and NMR spectroscopy. *Biochemistry* 37:18001–18009. doi:[10.1021/bi981046w](https://doi.org/10.1021/bi981046w)
- Zhai Y, Winter R (2013) Effect of molecular crowding on the temperature-pressure stability diagram of ribonuclease A. *ChemPhysChem* 14:386–393. doi:[10.1002/cphc.201200767](https://doi.org/10.1002/cphc.201200767)
- Zhang J, Peng XD, Jonas A, Jonas J (1995) NMR-study of the cold, heat, and pressure unfolding of ribonuclease-A. *Biochemistry* 34:8631–8641. doi:[10.1021/bi00027a012](https://doi.org/10.1021/bi00027a012)
- Zipp A, Kauzmann W (1973) Pressure denaturation of metmyoglobin. *Biochemistry* 12: 4217–4228

High Pressure Bioscience

Basic Concepts, Applications and Frontiers

Akasaka, K.; Matsuki, H. (Eds.)

2015, XVII, 730 p. 264 illus., 155 illus. in color.,

Hardcover

ISBN: 978-94-017-9917-1